frontiers in Plant Science

ORIGINAL RESEARCH
published: 12 June 2020
doi: 10.3389/fpls.2020.00794

High Photosynthetic Rates in a *Solanum pennellii* Chromosome 2 QTL Is Explained by Biochemical and Photochemical Changes

*Jaciara Lana-Costa[1], Franklin Magnum de Oliveira Silva[1], Willian Batista-Silva[1], Diego Costa Carolino[1], Renato Lima Senra[2], David B. Medeiros[1], Samuel Cordeiro Vitor Martins[1], Jorge Gago[3], Wagner L. Araújo[1] and Adriano Nunes-Nesi[1]**

[1] Departamento de Biologia Vegetal, Universidade Federal de Viçosa, Viçosa, Brazil, [2] Departamento de Bioquímica Aplicada, Universidade Federal de Viçosa, Viçosa, Brazil, [3] Departament de Biologia, Institute of Agro-Environmental Research and Water Economy – INAGEA, Universitat de les Illes Balears, Palma, Spain

OPEN ACCESS

Edited by:
Jose Luis Gonzalez Hernandez, South Dakota State University, United States

Reviewed by:
Elias Kaiser, Wageningen University & Research, Netherlands
Maria Manuela Rigano, University of Naples Federico II, Italy

***Correspondence:**
Adriano Nunes-Nesi
nunesnesi@ufv.br

Specialty section:
This article was submitted to Plant Breeding, a section of the journal Frontiers in Plant Science

Received: *25 February 2020*
Accepted: *19 May 2020*
Published: *12 June 2020*

Citation:
Lana-Costa J, de Oliveira Silva FM, Batista-Silva W, Carolino DC, Senra RL, Medeiros DB, Martins SCV, Gago J, Araújo WL and Nunes-Nesi A (2020) High Photosynthetic Rates in a Solanum pennellii Chromosome 2 QTL Is Explained by Biochemical and Photochemical Changes. Front. Plant Sci. 11:794. doi: 10.3389/fpls.2020.00794

Enhanced photosynthesis is strictly associated with to productivity and it can be accomplished by genetic approaches through identification of genetic variation. By using a *Solanum pennellii* introgression lines (ILs) population, it was previously verified that, under normal (CO_2), IL 2–5 and 2–6 display increased photosynthetic rates by up to 20% in comparison with their parental background (M82). However, the physiological mechanisms involved in the enhanced CO_2 assimilation exhibited by these lines remained unknown, precluding their use for further biotechnological applications. Thereby, here we attempted to uncover the physiological factors involved in the upregulation of photosynthesis in ILs 2–5 and 2–6 under normal (CO_2) as well as under elevated (CO_2). The results provide evidence for increased biochemical capacity (higher maximum carboxylation velocity and maximum electron transport rate) in plants from IL 2–5 and 2–6, whereas the diffusive components (stomatal and mesophyll conductances) were unaltered in these ILs in comparison to M82. Our analyses revealed that the higher photosynthetic rate observed in these ILs was associated with higher levels of starch as well as total protein levels, specially increased RuBisCO content. Further analyses performed in plants under high (CO_2) confirmed that biochemical properties are involved in genetic variation on chromosome 2 related to enhanced photosynthesis.

Keywords: photosynthesis, biochemical limitations, metabolism, tomato, growth

INTRODUCTION

Photosynthesis (*A*) is the main driving force for plant growth and biomass production having a central position for breeders seeking to increase crop yield (Evans, 2013; Nunes-Nesi et al., 2016; Nuccio et al., 2017; Batista-Silva et al., 2020; Flexas and Carriquí, 2020). The improvement of photosynthetic performance under optimal and suboptimal conditions can be accomplished by genetic approaches through identification of genetic variation, as well as selection of accessions

exhibiting higher photosynthetic rates. Moreover, understanding the mechanisms involved in the photosynthesis associated traits are required for improving the photosynthetic efficiency in crop species.

The photosynthetic efficiency can be enhanced, among others, by improving light capture through increasing pigment contents and by ameliorating light energy conversion (Ort et al., 2015). Furthermore, A can be improved by changes in stomatal properties (Rebetzke et al., 2013), ribulose 1,5 bisphosphate carboxilase oxigenase (RuBisCO) kinetic attributes (Parry et al., 2013), and also by modifying expression of others enzymes involved in carbon reduction reactions (Miyagawa et al., 2001; Lefebvre et al., 2005; Driever et al., 2017).

Alterations in A may be associated with diffusional limitations as those derived from changes in stomatal (g_s) and mesophyll (g_m) conductances which are dependent on leaf anatomical and physiological properties and influenced by environmental cues (Flexas et al., 2007, 2012; Vrabl et al., 2009; Galmés et al., 2011). For instance, high levels of CO_2 at the substomatal cavities (C_i) tend to reduce g_s in leaves by an intrinsic property of guard cells (Mott, 1988; Ainsworth and Rogers, 2007). Remarkably, at lower C_i, the maximum carboxylation velocity (V_{cmax}) limits photosynthesis. On the other hand, when C_i is higher, CO_2 assimilation is limited by maximum electron transport rate (J_{max}), or the regeneration of triose phosphate (Farquhar and Sharkey, 1982). Moreover, enrichment in the availability of atmospheric (CO_2) augments RuBisCO carboxylase activity leading to reduced photorespiratory process, improving carbon gains (Long et al., 2004; Peterhansel et al., 2010).

Natural genetic variation in diffusional and biochemical traits related to photosynthetic capacity have been verified in different plant species (Geber and Dawson, 1997; Galmés et al., 2014; Singh et al., 2014). For example, Mediterranean accessions of tomato (*S. lycopersicum*) cultivated under drought stress demonstrated higher transpiration efficiency provided by enchanced g_m/g_s ratio (Galmés et al., 2011). Furthermore, altered photosynthetic capacity can also be explained by components related to CO_2 assimilation capacity namely V_{cmax} and J_{max} (Dreyer et al., 2001; Driever et al., 2014; Walker et al., 2014). Thus, selection of accessions with higher J_{max} contributing to ribulose 1,5 bisphosphate (RuBP) regeneration has been proposed as a trait for plant breeding (Driever et al., 2014; Simkin et al., 2017a).

The use of introgression lines (ILs) populations, an important genomic tool for Quantitative Trait Locus (QTL) mapping, has been proposed to identify candidate genes associated with improved A (Flood et al., 2011; Gu et al., 2012; Nunes-Nesi et al., 2016). QTL analysis allow the identification of genomic regions where detailed studies should be performed to identify genes and nucleotide changes responsible for a certain function (Asín, 2002; Gonzalez-Martinez et al., 2006; Jamil et al., 2016; de Oliveira Silva et al., 2018). In a carbon isotope composition ($\delta^{13}C$) study performed with a *Solanum pennellii* population demonstrated that variation in stomatal arrangement may improve internal CO_2 diffusion allowing greater photosynthetic efficiency in dry environments (Xu et al., 2008; Muir et al., 2014). In addition, most of the genetic variation in tomato for g_s might be explained by differences in both width and anatomical traits of the stomatal pore (Fanourakis et al., 2015).

Recently, genomic regions involved in the regulation of photosynthesis and respiration were identified in tomato (de Oliveira Silva et al., 2018). In this study, a QTL for high A was identified in a unique overlapping genomic region, delimited by two ILs (IL 2–5 and IL 2–6) and named as BIN 2K. The IL 2–5 exhibited up to 20% increased A, 50% higher nitrate content and 21% higher starch accumulation at the end of the light period in comparison with the parental line M82. Similarly, the IL 2–6 exhibited 19% increased A, 22% higher g_s, 42% higher levels of starch at the end of the light period, and 58% higher starch turnover in comparison with M82. In agreement, the IL 2–6 also displayed higher g_s, when evaluating the variation in stomatal responsiveness to desiccation (Fanourakis et al., 2015). These two ILs were also evaluated for $\delta^{13}C$, in which IL 2–5 exhibited higher values of $\delta^{13}C$ compared to M82 and IL 2–6 (−28.1, −28.4, and −28.8, respectively) indicating increased water use efficiency (*WUE*) in this line (Xu et al., 2008). Notably, the IL 2–5 was also described as a drought-tolerant line mainly through alterations in organ morphogenesis and biochemical pathways (Gong et al., 2010). In addition, the IL 2–5, and IL 2–6 have also been characterized by exihibiting higher total plant weight, number of flower, fruits and seeds than M82 (Eshed and Zamir, 1995; Semel et al., 2006). However, the fruits from these ILs have reduced size and fresh weight when compared to M82 (Eshed and Zamir, 1995; Causse et al., 2004).

In order to investigate the physiological basis for the increased A associated with the genomic region BIN 2K, a detailed physiological characterization of the IL 2–5, IL 2–6, and M82 was performed under atmospheric and elevated (CO_2). Given that A is highly affected by environmental (CO_2) and RuBisCO limitation is reduced by high (CO_2; von Caemmerer and Farquhar, 1981), these ILs might exhibit higher carbon assimilation capacity under this condition. Our results demonstrate that the higher photosynthetic efficiency in the IL 2–5 and IL 2–6 was not associated with diffusive component (g_s and g_m), but rather to increased photobiochemical capacity. Our findings open important avenues for enhancing our understanding of genetic variation on chromosome 2 that is involved in the regulation of photosynthetic capacity in tomato plants.

MATERIALS AND METHODS

Plant Material and Experimental Conditions

Seeds of the ILs 2–5 and 2–6, as well as the cultivar M82 were sown in trays containing the commercial substrate Tropstrato HT, Vida Verde®. The plants were allocated in a greenhouse under naturally fluctuating conditions of light intensity (±600 μmol photons m^{-2} s^{-1} daily) and ambient CO_2 (±400 μmol mol^{-1}) as well as semicontrolled conditions of temperature (±28°C) and relative air humidity (±60%) during spring. After germination, seedlings were transplanted in 1.16 L pots containing the same commercial substrate, supplemented

with chemical fertilizer (N:4; P_2O_5:14; K_2O: 8) in the proportion of 0.5 kg of NPK to 10.0 kg of substrate. The plants were irrigated daily as needed and no restriction of root development, and consequently photosynthetic limitation, was observed at the end of the experiment when the physiological analyses and sample harvesting took place (4-week-old plants). Four plants for each genotype were grown side by side and the position of each plant was changed daily.

In a second experiment, seeds from the same genotypes were germinated and cultivated as described previoulsy with the following modifications. Pots containing plants with 10 days after transplanting (DAT) were transferred to open top chambers (OTCs) with the following specifications 1.6 m diameter and 1.8 m height. The chambers were placed in a greenhouse under naturally fluctuating conditions of light intensity (±600 μmol photons m^{-2} s^{-1} daily) and ambient CO_2 (±400 μmol mol^{-1}) as well as semicontrolled conditions of temperature (±28°C) and relative air humidity (±60%). The experiment was carried out in two OTCs. One was continuously maintained at the current ambient level of CO_2 (∼400 μmol mol^{-1}) and another continuously maintained at an elevated level of CO_2 (∼800 μmol mol^{-1}). In the chamber supplemented with elevated (CO_2), 800 μmol mol^{-1} was the setpoint and the (CO_2) was monitored and adjusted every day with a portable CO_2 meter AZ-77535. CO_2 was only injected following the photoperiod, i.e., from 06:00 a.m. to 06:00 p.m. The obtained (CO_2) along the experiments are presented in **Supplementary Figure S1**. Air temperature averages (±30°C) and relative air humidity (±77%) inside the OTCs were measured throughout the experiment and did not differ significantly between the two sets of OTCs during the experiment. The two OTCs were installed at 1 m of distance between each other. The plants remained under these conditions for 3 weeks until further analysis. Four plants for each genotype were grown inside each chamber and the positions of the plants inside the chamber were daily changed.

Growth and Fruit Analyses

Growth parameters were determined in 4-week-old plants. Total leaf area was measured using a LI-3100C Area Meter (LiCor, Lincoln, NE, United States) while specific leaf area (SLA) was measured as described previously (Hunt et al., 2002). The dry matter accumulated in leaves, stems and roots were determined as described previously (de Oliveira Silva et al., 2018). Total fruit production was determined at the end of the cultivation in plants with 60 DAT. The fruits were harvested when they presented the reddish color, characteristic of mature fruits. We determined the total number of fruits per plant, the mean fruit fresh weight per plant as well as the fruit size, by measuring the fruit length, and diameter using a digital caliper.

Measurements of Gas Exchange Parameters and Chlorophyll *a* Fluorescence

Gas exchange and chlorophyll *a* fluorescence analyses were performed simultaneously using an open-flow infrared gas exchange analyzer system equipped with an integrated fluorescence chamber (IRGA, LI-COR Inc. LI-6400XT; NE). These analyses were realized during the light period, from 8 h to 12 h (solar time) using the 2 cm^2 leaf chamber at 25°C, flow rate of 300 mol s^{-1}, 0.5 stomatal ratio (amphistomatic leaves), and saturating light intensity of 1,000 μmol photons m^2 s^{-1}. The leaf-to-air vapor pressure deficit ranged from 1.2 to 2.0 kPa and the amount of blue light was set to 10% of photosynthetic photon flux density (PPFD) to optimize stomatal aperture. The initial fluorescence (F_0) was measured in illuminating dark-adapted leaves (for at least 1 h) with weak modulated measuring beams (0.03 μmol m^{-2} s^{-1}). A saturating white light pulse (8,000 μmol m^{-2} s^{-1}) was applied for 0.8 s to obtain the maximum fluorescence (F_m), from which the variable-to-maximum Chl fluorescence ratio was then calculated: $F_v/F_m = [(F_m - F_0)/F_m)]$. In light-adapted leaves, the steady-state fluorescence yield was measured with the application of a saturating white light pulse (8,000 μmol m^{-2} s^{-1}) to achieve the light adapted maximum fluorescence ($F_{m'}$). A far-red illumination (2 μmol m^{-2} s^{-1}) was applied after turn off the actinic light to measure the light-adapted initial fluorescence ($F_{0'}$). The capture efficiency of excitation energy by open PSII reaction centers ($F_{v'}/F_{m'}$) was estimated following a previously described procedure (Logan et al., 2007) and the actual PSII photochemical efficiency (φPSII) was estimated as $\varphi PSII = (F_{m'} - F_s)/F_{m'}$ (Genty et al., 1989). Electron transport rate (ETR) was calculated as follows: $\phi PSII \times PARi \times \beta \times \alpha$, where PARi is the incident radiation, β is the absorbed quanta partition factor between PSII/I (assumed to be 0.5), and α is the leaf absorbance. Leaf absorbance (α) was estimated by the chlorophyll content per unit area as follow: $\alpha = \chi/(\chi + 76)$, where χ is the chlorophyll content per unit area (Evans and Poorter, 2001).

From combined measurements of fluorescence and gas exchange, we estimated the photorespiration rate (P_r) according to Valentini et al. (1995). Dark respiration rate (R_d) was measured by the same gas exchange system after plants being at least 2 h into the dark period.

Photosynthetic light-response curves (*A*/PPFD) were performed using atmospheric (CO_2; C_a) of 400 μmol CO_2 mol^{-1} and the plants were exposed to a range of PPFD in the sequence: 1,000, 1,500, 1,300, 1,100, 1,000, 800, 600, 400, 300, 200, 100, 50, and 0 μmol photons m^{-2} s^{-1}. Variables derived from the *A*/PPFD curves were estimated from adjustments of light response curve by the non-rectangular hyperbolic model (von Caemmerer, 2000). Measurements for CO_2 response curves were taken at light saturation point of 1,000 μmol m^2 s^{-1}, 25°C at atmospheric CO_2 concentration (C_a) of 400 μmol mol^{-1} and once the steady state was reached, the C_a was decreased to 300, 200, 100, and 50 μmol mol^{-1}. Then, C_a was increased to 400, 500, 600, 800, 1,000, 1,200, 1,400, and 1,600 μmol mol^{-1}. Curves were obtained using the second terminal leaflet of the third fully expanded leaf from the apex of 4—week—old plants.

For the high (CO_2) experiments, instantaneous gas exchange and chlorophyll *a* fluorescence analyses were performed as previously described, with minor modifications. All measurements were performed during the light period between 8 h and 12 h (solar time) under 1,000 μmol photons m^{-2} s^{-1}

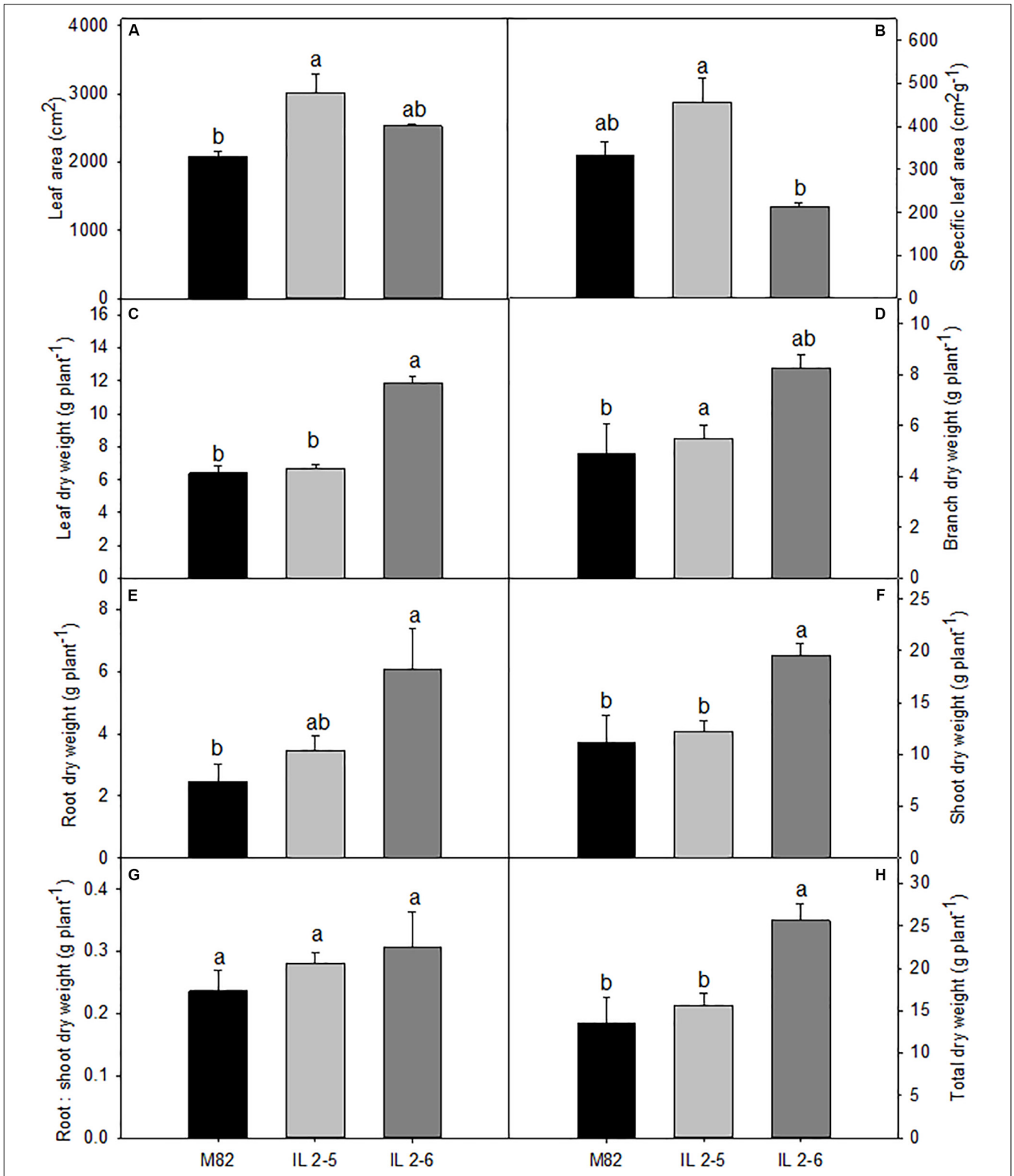

FIGURE 1 | Growth phenotypes of 4–week–old plants from two ILs of *Solanum pennellii* into a genetic background of *Solanum lycopersicum* (M82) grown at 400 μmol CO_2 mol^{-1}. Total leaf area **(A)**; Specific leaf area **(B)**; Leaf dry weight **(C)**; Branch dry weight **(D)**; Root dry weight **(E)**; Shoot dry weight **(F)**; Root: shoot dry weight ratio **(G)**; and Total dry weight **(H)**. Values are presented as means ± *SE* (n = 4). Different letters accompany means that differ between the genotypes ($P < 0.05$) by the Tukey test.

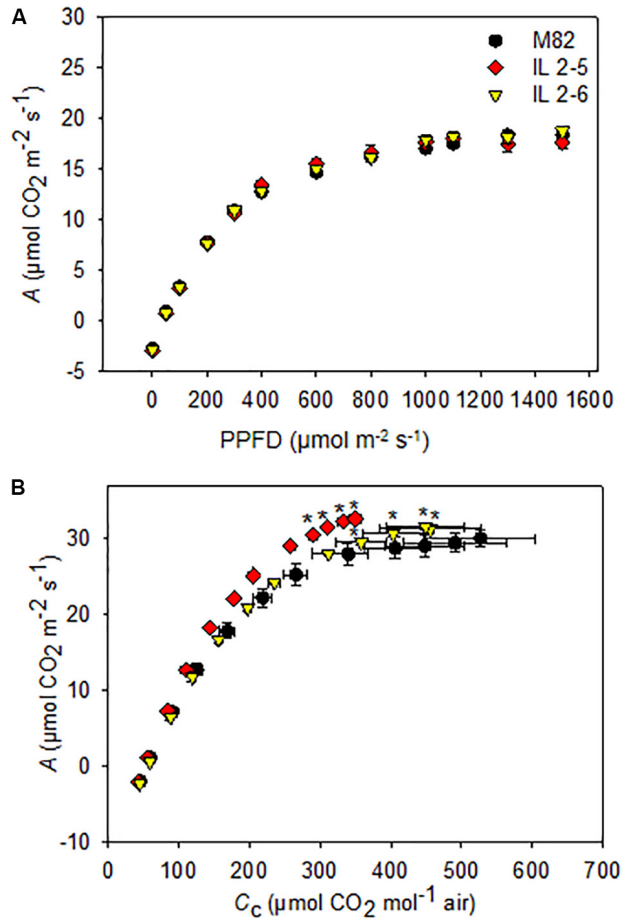

FIGURE 2 | Photosynthesis response curves to photosynthetic photon flux density (*A*/PPFD) and chloroplastidic CO_2 (A/C_c) of 4–week–old plants from two ILs of *Solanum pennellii* into a genetic background of *Solanum lycopersicum* (M82) grown at 400 µmol CO_2 mol^{-1}. *A*/PPFD **(A)**; A/C_c **(B)**. Values are presented as means ± *SE* (n = 4). Asterisks indicate differences of the ILs in relation to M82 ($P < 0.05$) according to the Tukey test.

at the leaf level (light saturation) of PPFD, determined by *A*/PPFD curves and at 25°C. The reference (CO_2) was set at 400 µmol mol^{-1} for plants at atmospheric (CO_2) and 800 µmol mol^{-1} for plants under elevated (CO_2). Instantaneous measurements were obtained using the second terminal leaflet of the third fully expanded leaf from the apex of 4−week−old plants. R_d was determined as described previously.

Estimation of Mesophyll Conductance (g_m), Maximum Rate of Carboxylation (V_{cmax}), Maximum Rate of Electron Transport (J_{max}), and Photosynthetic Limitations

The concentration of CO_2 in the carboxylation sites (C_c) was calculated following Harley et al. (1992) as $gm = A / \left[Ci - (\Gamma^* (ETR + 8(A + Rd)))/(ETR - 4(A + Rd))\right]$, and using Γ^* for tomato measured previously (Hermida-Carrera et al., 2016). The g_m data were employed to convert the A–C_i curves into A–C_c curves using the following equation $C_c = C_i - (A/g_m)$. ETR calculation using the proxy of α estimation, by the chlorophyll content empirical equation (Evans and Poorter, 2001), was additionally checked through a sensitivity analysis to ensure that the possible variability in α do not affect g_m estimates. Values for g_m were also estimated by the Ethier and Livingston (2004) method.

The parameters from A/C_c in plants under ambient (CO_2), as V_{cmax} and J_{max} were calculated by fitting the mechanistic model of CO_2 assimilation (Farquhar et al., 1980), using the C_c based on temperature of kinetic parameters of RuBisCO (K_c and K_o). V_{cmax}, J_{max}, and g_m were normalized to 25°C using the temperature response and plug-in equations described by Sharkey et al. (2007). For the second experiment, the V_{cmax} single point was only calculated for plants growing under atmospheric (CO_2; 400 µmol mol^{-1}; De Kauwe et al., 2016).

Values of A, g_s, g_m, and ETR were employed to calculate the quantitative photosynthesis limitation analysis as described by Grassi and Magnani (2005) that permits the partitioning into the functional components of photosynthetic constraints related to stomatal (l_s), mesophyll (l_m), and leaf biochemical (l_b) limitations. According to A–C_c curves obtained in the firt experiment, photosynthesis at the growing (CO_2) was found at the curvi-linear part of the response, associated to the energy limited RuBP regeneration (J_{max}). Since ETR is tightly coupled to J_{max}, and should reflect gross photosynthesis (Genty et al., 1989; Valentini et al., 1995), calculations of l_b were confirmed using ETR as a surrogate for leaf biochemistry (Galle et al., 2009; Pons et al., 2009).

Metabolite Analyses

Samples from fully expanded leaves were harvested in five different time points (beginning, middle and end of the light period, and as well as middle and end of the dark period) for the first experiment and two different time points (middle of the light period and end of the dark period) for the second experiment from 4−week−old plants. The material was frozen in liquid nitrogen and stored at -80°C for further analyses. Samples were homogenized and aliquots of approximately 20 mg were subjected to hot ethanol extraction as described by Cross et al. (2006). The levels of starch, glucose, fructose, and sucrose were measured as described by Fernie et al. (2001). The levels of chlorophyll (*a* and *b*) were determined exactly as previously described (Porra et al., 1989). Nitrate contents were determined as detailed by Sulpice et al. (2009) and malate and fumarate as Nunes-Nesi et al. (2007). The total protein was measured according by Bradford (1976) and the total amino acids content was determined using a colorimetric assay according to Yemm et al. (1955).

Protein Extraction and Western Blot Analysis

Total soluble protein was extracted from 200 mg (fresh weight) of leaf tissue according to the protocol of Vasconcelos et al. (2005)

TABLE 1 | Photosynthetic characterization of 4−week−old plants from two ILs of *Solanum pennellii* into a genetic background of *Solanum lycopersicum* (M82) grown at 400 μmol CO_2 mol^{-1}.

Parameters	M82	IL 2–5	IL 2–6
A (μmol CO_2 m^{-2} s^{-1})	22.80 ± 0.54**a**	21.46 ± 0.65**a**	22.67 ± 0.73**a**
A_{gross} (μmol CO_2 m^{-2} s^{-1})	33.15 ± 1.33**b**	37.35 ± 0.99**ab**	37.93 ± 0.51**a**
R_d (μmol CO_2 m^{-2} s^{-1})	2.70 ± 0.12**a**	3.09 ± 0.24**a**	3.48 ± 0.33**a**
P_r (μmol CO_2 m^{-2} s^{-1})	7.64 ± 1.035**b**	12.80 ± 0.553**a**	11.77 ± 0.281**a**
ETR (μmol e^- m^{-2} s^{-1})	188.18 ± 13.12**b**	241.32 ± 5.522**a**	237.48 ± 2.50**a**
g_s (mol CO_2 m^{-2} s^{-1} Pa^{-1})	0.220 ± 0.051**a**	0.205 ± 0.021**a**	0.223 ± 0.096**a**
g_m_Harley (mol m^{-2} s^{-1} Pa^{-1})	0.188 ± 0.015**a**	0.134 ± 0.020**a**	0.172 ± 0.029**a**
g_m_Ethier (mol m^{-2} s^{-1} Pa^{-1})	0.205 ± 0.019**a**	0.211 ± 0.027**a**	0.219 ± 0.017**a**
C_c (μmol CO_2 mol^{-1})	175.17 ± 17.04**a**	119.522 ± 3.34**b**	127.77 ± 4.61**b**
V_{cmax}_C_c (μmol m^{-2} s^{-1})	135.68 ± 12.45**b**	225.15 ± 19.75**a**	206.25 ± 13.36**a**
J_{max}_C_c (μmol m^{-2} s^{-1})	159.50 ± 9.66**b**	228.99 ± 12.20**a**	220.28 ± 9.69**a**
l_s	0.271 ± 0.007**a**	0.272 ± 0.013**a**	0.250 ± 0.013**a**
l_m	0.408 ± 0.030**a**	0.484 ± 0.023**a**	0.459 ± 0.039**a**
l_b	0.319 ± 0.030**a**	0.243 ± 0.015**a**	0.290 ± 0.029**a**

*These data are derived from A/C_c response curve shown in **Figure 2B** at ambient CO_2 concentration (C_a) of 400 μmol mol^{-1} setpoint. Measurements of photosynthetic carbon fixation rates were determined at saturating-light levels of 1,000 μmol m^{-2} s^{-1} in the second terminal leaflet of the third fully expanded leaf from ILs and M82 plants. Values are presented as means ± SE (n = 4). Different letters accompany means that differ between the genotypes ($P < 0.05$) by the Tukey test. A, net CO_2 assimilation rate; A_{gross}, $A + P_r + R_d$; R_d, dark respiration; P_r, photorespiration; ETR, electron transport rate; g_s, stomatal conductance; g_m, mesophyll conductance to CO_2; C_c, chloroplastic CO_2 concentration; V_{cmax}_C_c, maximum carboxylation velocity based on C_c; and J_{max}_C_c, maximum capacity for electron transport rate based on C_c; l_s, stomatal limitation; l_m, mesophyll limitation; and l_b, biochemical limitation.*

and quantified using the Bradford method (Bradford, 1976). Forty micrograms of total protein was subjected to a solution containing sample buffer (125 mM Tris–HCl, pH 6.8, containing SDS 4%, 20% glycerol, 4% 2-mercaptoethanol, and 0.1% bromophenol blue). The samples were separated using 12% glycine sodium dodecyl sulfate polyacrylamide gel electrophoresis (Glycine–SDS-PAGE). The proteins were electrophoretically transferred to nitrocellulose membrane (0.45 μm; Bio-Rad) by the method of Towbin et al. (1979). The membranes were blocked for 2 h with 3% (w/v) Bovine serum albumin in Tris–buffered saline (2 M Tris–HCl, pH 7.4, containing 5 M NaCl, and 10% tween). The blots were then incubated for 2 h with specific antibodies raised in rabbit (serum diluted 1:12000 large subunit – AS03 037 code). The membranes were treated for 2 h with bridging antibodies (Anti-rabbit HRP-conjugated secondary antibodies GE Healthcare, RPN2108 code) diluted 1:10000. Large RuBisCO subunit was visualized with substrate solution (10 mg of 3,3' -Diaminobenzidine mixed with 10 mL of Tris–buffered saline and 10 μL of H_2O_2). All steps were performed at room temperature. Tween-20 in Tris–buffered saline was used for washing (five times for 5 min between all treatments mentioned above) as well as for the dilution of antibodies. The bands on immunoblots were quantified by densitometry using the semi-quantitative ImageJ software (Version 1.1.4) as previously described (Tiranti et al., 2009; Brandt et al., 2018). Data were normalized by standard marker (∼50 kDa) and expressed in fold change.

Statistical Analyses

The experiments were performed in a randomized complete block design. The data of the two experiments was submitted to analysis of variance (ANOVA). In the second experiment, two levels of the same categorical variable (CO_2 environment) were considered. The variability of the results is expressed as the mean ± standard error (SE) of n independent biological replicates. Four biological replicates ($n = 4$) were utilized for each analysis, except for Western blot, where three biological replicate ($n = 3$) were analyzed. In order to verify the statistical difference between the genotypes, the means were compared using the Tukey test ($P < 0.05$). Pearson correlation matrices were performed to determine the correlated structure of the different parameters which were considered to be significant when $P < 0.05$. All analyses were performed using the GENES program (Cruz, 2013).

RESULTS

Growth-Related Parameters

In order to evaluate growth related phenotypes, ILs 2–5, 2–6, and M82 plants were grown side by side in a greenhouse. Detailed examination revealed that both ILs tended to perform better than M82, whereas IL 2–5 exhibited increased total leaf area (**Figure 1A**), IL 2–6 displayed higher total dry weight (**Figure 1H**). Despite certain differences in leaf, branch, and root dry weights (**Figures 1C–E**), no alteration in biomass allocation was observed, as indicated by similar root:shoot ratios in all genotypes (**Figure 1G**).

Photosynthesis Related Parameters

Since the ILs 2–5 and 2–6 previously showed higher photosynthetic rate (de Oliveira Silva et al., 2018), we decided to investigate the photosynthetic capacity of these ILs by varying

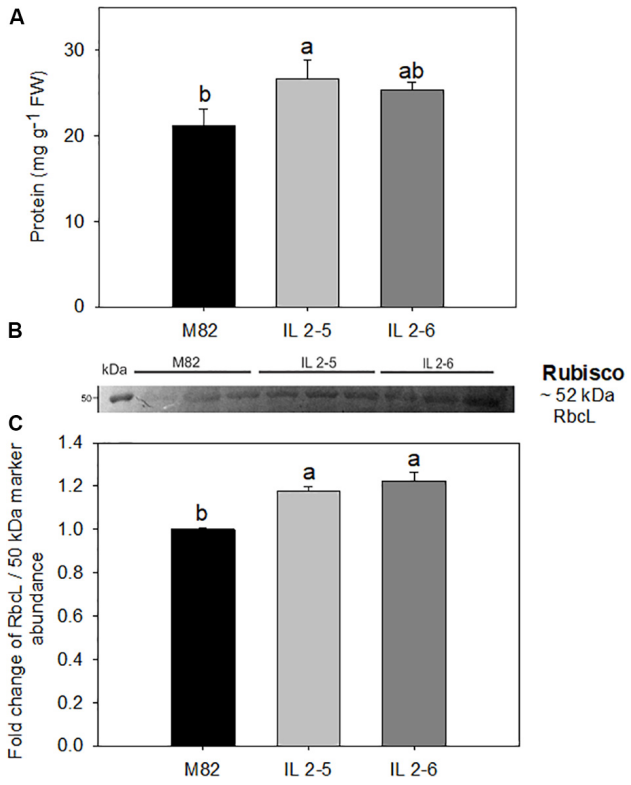

FIGURE 3 | Protein content and RuBisCO large subunit (RbcL) in 4–week–old plants from two ILs of *Solanum pennellii* into a genetic background of *Solanum lycopersicum* (M82) grown at 400 μmol CO_2 mol^{-1}. Protein **(A)**; Levels of RbcL determined by Western blot **(B)**; and quantification of western blot results **(C)**. Values for protein are presented as means ± *SE* (*n* = 4). Values for Western blot are expressed as fold change over the control M82 and presented as means ± *SE* (*n* = 3). Signal intensities were measured using ImageJ software and normalized to the amount of loaded marker (~50 kDa). Different letters accompany means that differ between the genotypes ($P < 0.05$) by the Tukey test. FW: Fresh weight.

light intensity. We found a similar *A* response to different light intensities in all genotypes (**Figure 2A**), therefore no differences for light saturation and compensation points were observed (**Supplementary Table S1**).

We next characterized *A* in these lines under variable CO_2 concentrations by performing A/C_c curve analysis. First, there were no differences in calculations on C_i basis (data not shown) but only on C_c. Therefore, it was necessary to carry out a complete photosynthetic study of the calculations considering the g_m, including to evaluate the photosynthetic limitations for each of the lines. Interestingly, increased photosynthetic rates were observed under specific conditions for the two ILs (**Figure 2B**). From A/C_c curves, both ILs displayed higher CO_2 assimilation rate at the final point of the curve when compared to M82 (**Figure 2B**).

Concerning photosynthetic characterization of plants under atmospheric (CO_2; **Table 1**), further analyses indicated that plants from the two ILs displayed similar *A*, R_d, g_s, and g_m. On the other hand, IL 2–6 displayed increased gross photosynthesis (A_{gross}) and both ILs higher P_r, ETR and lower chloroplastic CO_2 concentration (C_c), probably due to the higher carboxylation demand, driven by the maximum RuBisCO carboxylation velocity based on C_c ($V_{cmax}\_C_c$). In addition, the J_{max} was higher in the ILs in comparison to M82.

Protein and RuBisCO Content in Leaves

The total protein levels were consistently increased by up to 21% in the IL 2–5 in comparison to M82 cultivar (**Figure 3A**). Thus, we next analyzed the levels of RuBisCO via western blot with antibodies against its large subunit (RbcL; **Figures 3B,C** and **Supplementary Figure S3**). By quantifying the band intensity, we verified a significant increase (~20%) in the levels of RbcL in both ILs compared to M82 (**Figure 3C**).

Diurnal Pattern of Metabolite Levels in Leaves

Increased starch content in leaves at the end of the light period in the ILs 2–5 and 2–6 was observed when compared to M82 (**Figure 4A**). On the other hand, at the end of dark period, the starch levels were reduced in IL 2–6, indicating higher starch degradation during the night period (**Figure 4A**). The glucose levels were increased at the end of the light period and sucrose showed lower levels in the middle of the night in the IL 2–5 compared to M82 (**Figures 4B,D**). Regarding the levels of fructose, we did not observe differences among the three genotypes (**Figure 4C**). The levels of malate and fumarate were generally similar to those observed in leaves of M82, except for a reduction in malate levels at the beginning of the day (**Figures 4E,F**) and in fumarate at the end of the night. Total chlorophyll and amino acids as well as nitrate levels did not differ among genotypes (**Supplementary Figures S2A,C,D**).

Fruit Related Parameters

We also evaluated whether the greater photosynthetic efficiency would reflect on total fruit production (**Supplementary Figure S4**). We observed that plants from IL 2–5 produced greater number of fruits with 88% more fruits than M82 plants (**Supplementary Figure S4A**). However, both ILs produced smaller fruits than M82 plants, which resulted in no differences in total fruit fresh weight per plant between ILs and M82 (**Supplementary Figures S4B–D**).

Elevated (CO_2) Modifies Photosynthetic Parameters as Well as Carbon and Nitrogen Metabolism in Tomato ILs

Given the increased photosynthetic capacity observed in the ILs, indicated by the higher assimilation rate at saturating (CO_2), we comparatively analyzed plants from M82 and the two ILs growing for 3 weeks under atmospheric and elevated (CO_2). We noticed under the OTC conditions, which are slightly different from the greenhouse conditions, such as higher air temperature and relative air humidity, a minor decrease in the photosynthetic capacity of all genotypes as they exhibited lower A_{gross} and ETR (**Table 2**). However, the ILs still displayed higher ETR, V_{cmax} values (**Table 2**), and protein content (IL 2–5; **Figure 6B**),

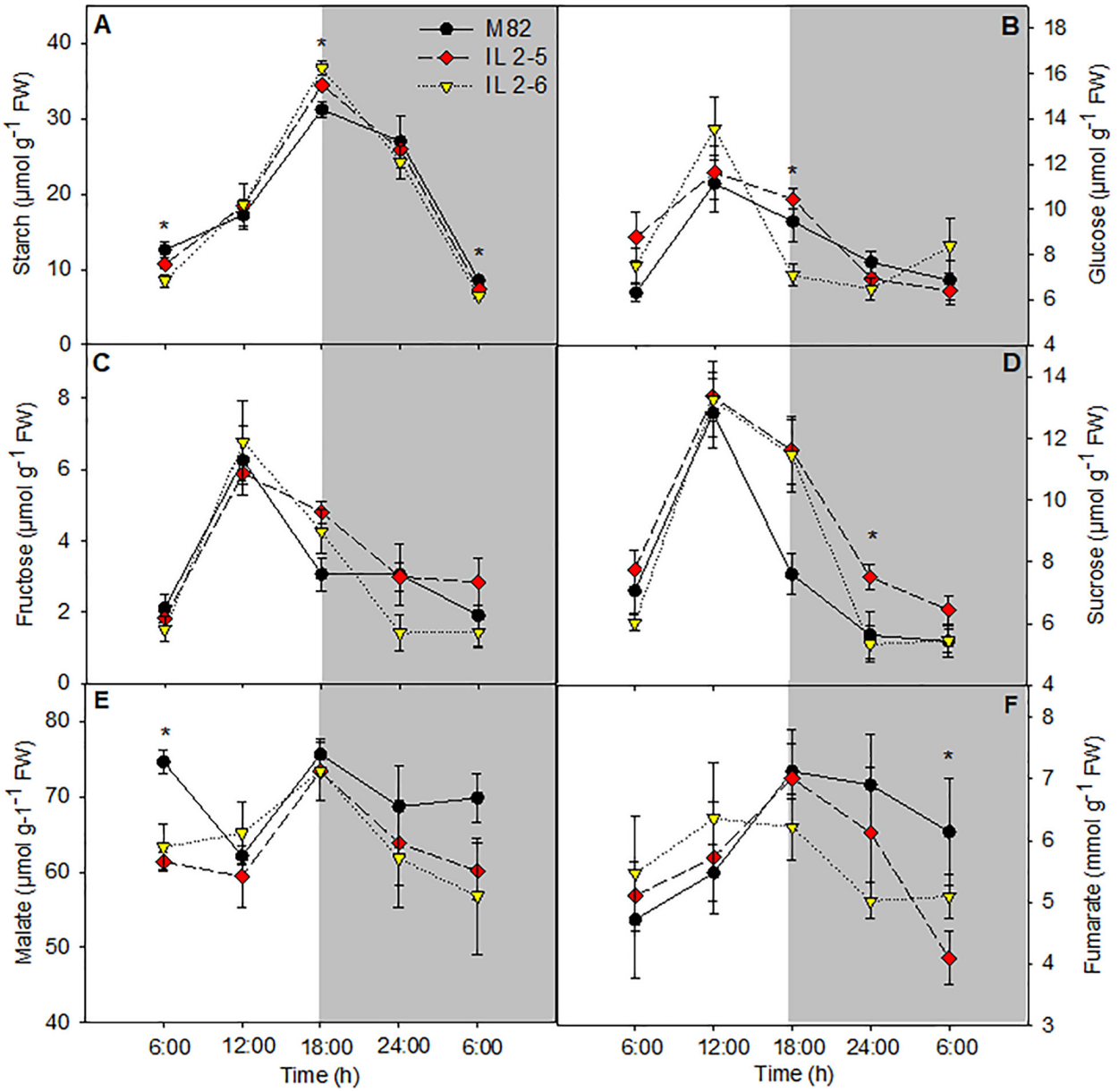

FIGURE 4 | Changes in the metabolite contents involved in carbon metabolism of 4–week–old plants from two ILs of *Solanum pennellii* into a genetic background of *Solanum lycopersicum* (M82) grown at 400 µmol CO_2 mol^{-1}. Starch **(A)**; Glucose **(B)**; Fructose **(C)**; Sucrose **(D)**; Malate **(E)**; and Fumarate **(F)**. Values are presented as means ± *SE* (n = 4). Asterisks indicate differences of the ILs in relation to M82 ($P < 0.05$) according to the Tukey test. FW: Fresh weight.

confirming the superior photobiochemistry capacity of these ILs in comparison to M82 plants. Under elevated (CO_2), an increase of 22% in assimilation rate was observed in the ILs in comparison to M82 plants (**Table 2**). In addition, A_{gross}, P_r, and ETR were significantly higher in the ILs at high (CO_2; **Table 2**). No changes were observed for R_d, g_s, and g_m at high (CO_2) among ILs and M82 plants (**Table 2**). Whereas stomatal limitation was increased in the IL 2–5, biochemical limitation decreased in both ILs at elevated (CO_2; **Table 2**).

To further understand the physiological advantage provided by increased photobiochemistry in the ILs, we explored the relationship between diffusive and biochemical limitations (l_d/l_b) with A and ETR comparing ILs to M82 as well as the two growing conditions [400 and 800 ppm (CO_2)] (**Figure 5**). At 400 ppm (CO_2), as expected diffusive limitations were double than biochemicals ($l_d/l_b > 2$) where ILs obtained higher A mostly due to lower biochemical limitation (thus promoted higher l_d/l_b ratio than M82; **Figure 5A**) in comparison to M82. However, under 800 ppm (CO_2) diffusive limitations became less important with all limitations highly balanced ($l_d/l_b \sim 1$), and again ILs even at high (CO_2) showed biochemical limitations more reduced than diffusive ones (thus promoted higher l_d/l_b ratio than M82) when

TABLE 2 | Photosynthetic characterization of 4−week−old plants from two ILs of *Solanum pennellii* into a genetic background of *Solanum lycopersicum* (M82) grown at 400 and at 800 μmol CO_2 mol^{-1}.

	400 μmol CO_2 mol^{-1}			800 μmol CO_2 mol^{-1}		
Parameters	**M82**	**IL 2–5**	**IL 2–6**	**M82**	**IL 2–5**	**IL 2–6**
A (μmol CO_2 m^{-2} s^{-1})	18.32 ± 0.610**Aa**	20.16 ± 0.787**Aa**	20.14 ± 0.622**Aa**	18.07 ± 1.06**Ba**	22.06 ± 1.552**Aa**	21.84 ± 0.711**Aa**
A_{gross} (μmol CO_2 m^{-2} s^{-1})	25.29 ± 0.876**Aa**	29.10 ± 1.30**Aa**	29.36 ± 0.99**Aa**	21.83 ± 1.07**Ba**	28.604 ± 1.85**Aa**	27.18 ± 0.80**Aa**
R_d (μmol CO_2 m^2 s^{-1})	1.67 ± 0.101**Aa**	1.91 ± 0.181**Aa**	1.65 ± 0.080**Aa**	1.68 ± 0.140**Aa**	1.51 ± 0.275**Aa**	1.729 ± 0.058**Aa**
P_r (μmol CO_2 m^{-2} s^{-1})	5.32 ± 0.439**Ba**	7.02 ± 0.364**Aa**	7.57 ± 0.436**Aa**	2.07 ± 0.127**Bb**	5.01 ± 0.670**Ab**	3.60 ± 0.166**Ab**
ETR (μmol e^- m^{-2} s^{-1})	139.48 ± 6.017**Ba**	170.42 ± 7.215**Aa**	173.01 ± 7.449**Aa**	98.69 ± 3.944**Bb**	151.53 ± 11.187**Aa**	135.73 ± 3.638**Ab**
g_s (mol CO_2 m^{-2} s^{-1} Pa^{-1})	0.229 ± 0.029**Aa**	0.248 ± 0.018**Aa**	0.241 ± 0.012**Aa**	0.233 ± 0.037**Aa**	0.187 ± 0.036**Aa**	0.219 ± 0.056**Aa**
g_m (mol CO_2 m^{-2} s^{-1} Pa^{-1})	0.170 ± 0.018**Aa**	0.171 ± 0.0301**Aa**	0.158 ± 0.008**Aa**	0.072 ± 0.006**Ab**	0.071 ± 0.007**Ab**	0.068 ± 0.007**Ab**
C_c (μmol CO_2 mol^{-1})	194.38 ± 10.42**Ab**	165.88 ± 1.06**Ab**	159.22 ± 4.15**Ab**	402.42 ± 15.75**Aa**	234.01 ± 24.59**Ca**	303.00 ± 11.18**Ba**
V_{cmax}_C_c (μmol m^{-2} s^{-1})	111.83 ± 6.45**B**	154.78 ± 5.30**A**	160.90 ± 7.46**A**	–	–	–
l_s	0.383 ± 0.030**Aa**	0.418 ± 0.038**Aa**	0.421 ± 0.013**Aa**	0.159 ± 0.038**Bb**	0.329 ± 0.047**Aa**	0.247 ± 0.056**ABb**
l_m	0.386 ± 0.020**Aa**	0.401 ± 0.034**Ab**	0.408 ± 0.028**Aa**	0.525 ± 0.037**Aa**	0.525 ± 0.037**Aa**	0.489 ± 0.051**Aa**
l_b	0.230 ± 0.038**Ab**	0.180 ± 0.010**Aa**	0.169 ± 0.016**Aa**	0.416 ± 0.065**Aa**	0.181 ± 0.028**Ba**	0.262 ± 0.018**Ba**

Measurements of photosynthetic carbon fixation rates were determined at ambient and elevated CO_2 concentration (C_a) of 400 μmol mol^{-1} and 800 μmol mol^{-1}, respectively, and at saturating-light levels of 1,000 μmol m^{-2} s^{-1} in the second terminal leaflet of the third fully expanded leaf from ILs and M82 plants. Values are presented as means ± SE (n = 4). Capital letters compare means that differ between the genotypes within a treatment ($P < 0.05$) by the Tukey test. Lowercase letters compare means that differ in a single genotype between the two treatments ($P < 0.05$) by the Tukey test. A, Assimilation rate; A_{gross}, $A + P_r + R_d$; R_d, dark respiration; P_r, photorespiration; ETR, electron transport rate; g_s, stomatal conductance g_m, mesophyll conductance to CO_2 estimated according to the Harley method; C_c, chloroplastic CO_2 concentration; V_{cmax}_ C_c, maximum carboxylation velocity single point based on C_c; l_s, stomatal limitation; l_m, mesophyll limitation; and l_b, biochemical limitation.

compared to M82 (**Figure 5A**). The very same trend observed for the gas-exchange *A* parameter was observed for the fluorescence ETR value where ILs showed higher values than M82 at both growing conditions (**Figure 5B**).

We next analyzed the levels of the major leaf metabolites in the ILs under elevated (CO_2; **Figure 6**). In agreement with previous results suggesting higher photosynthetic efficiency of both ILs above 800 ppm (CO_2), significant increase in the total chlorophyll (IL 2–5), and protein contents (IL 2–5) at the middle of the day, as well as fructose (both ILs) at the end of the dark period was verified (**Figures 6A,B,E**). Whilst sucrose at the end of the dark period increased in IL 2–5, it was reduced in IL 2–6 in ambient and elevated (CO_2) compared to M82 (**Figure 6F**). On the other hand, glucose, fructose, and sucrose, total amino acids, and malate contents were unaltered at the middle of the light period in both ambients (**Figures 6D–F** and **Supplementary Figures S5B,C**). Similar to the previous observations under atmospheric (CO_2), an increase in starch levels was observed in

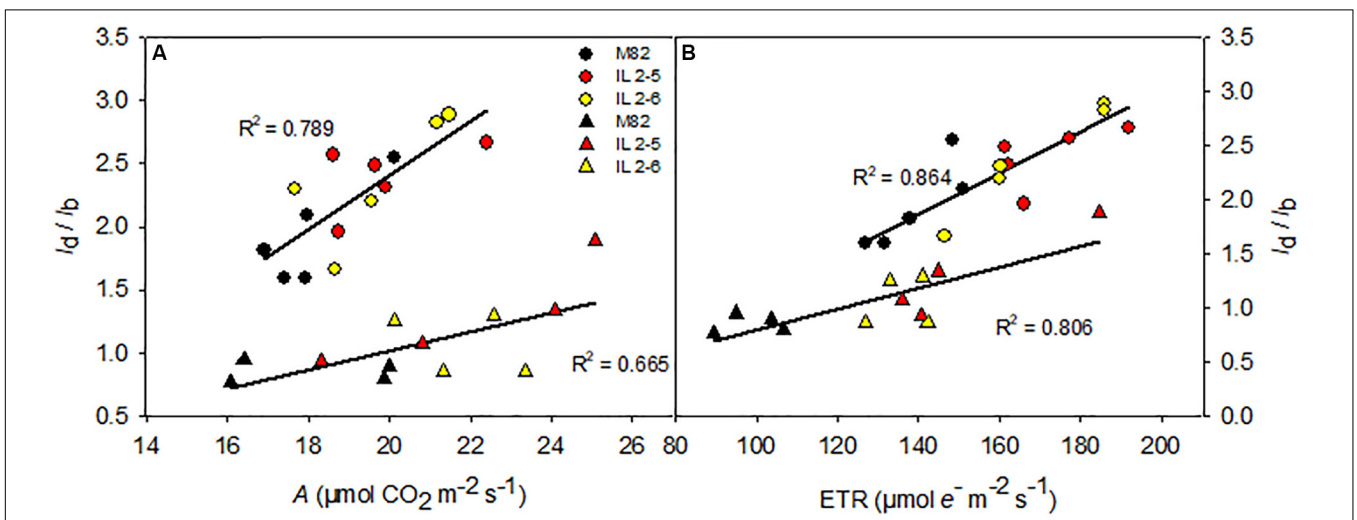

FIGURE 5 | Relationships between the ratio between diffusive and biochemical photosynthetic limitations (l_d/l_b) and photosynthesis (*A*; **A**) and electron transport rate (ETR; **B**) of 4-week-old plants from two ILs of *Solanum pennellii* into a genetic background of *Solanum lycopersicum* (M82) grown at 400 and at 800 μmol CO_2 mol^{-1}. The l_d/l_b is the ratio between the diffusive limitations ($g_s + g_m$) divided by the biochemical limitations. g_s and g_m, stomatal conductance and mesophylic conductance, respectively. Each point represents biological replicate. Circle symbol indicates genotypes cultivated under ambient (CO_2) in the legend and triangle symbol, elevated (CO_2). All correlations are significant at $P < 0.005$. R^2: determination coefficient.

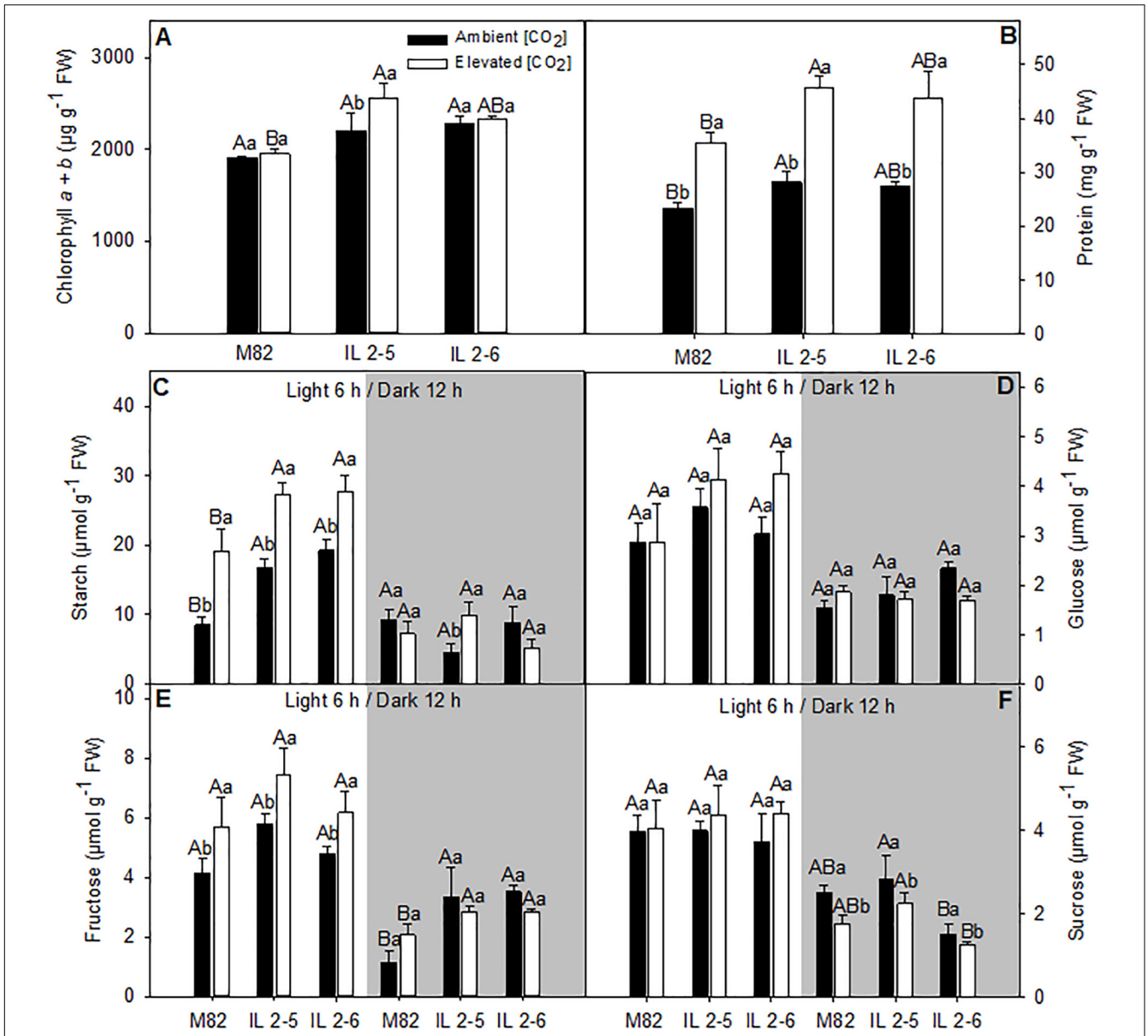

FIGURE 6 | Metabolite levels of 4–week–old plants from two ILs of *Solanum pennellii* into a genetic background of *Solanum lycopersicum* (M82) grown at 400 and at 800 µmol CO_2 mol^{-1}. Metabolite levels were measured in leaves at the middle of the light period (white sectors) and the end of dark period (gray sectors). Chlorophyll *a* + *b* **(A)**; Protein **(B)**; Starch **(C)**; Glucose **(D)**; Fructose **(E)**; and Sucrose **(F)**. Values are presented as means ± *SE* (*n* = 4). Capital letters compare means that differ between the genotypes within a treatment ($P < 0.05$) by the Tukey test. Lowercase letters compare means that differ in a single genotype between the two treatments ($P < 0.05$) by the Tukey test. FW: Fresh weight.

plants from both ILs compared to M82 at the middle of the light period (**Figure 6C**). Noteworthy, there was an increase in starch levels at the middle of the light period in all genotypes under elevated (CO_2), nevertheless the ILs exhibited higher starch levels in relation to M82 (**Figure 6C**).

Pearson correlation analysis was applied to further comprehend how metabolic changes and structural components are driving *A* in the ILs (**Supplementary Figure S6**). No significant correlation was observed relating *A* and general leaf biochemical and structural parameters as total chlorophyll and protein content at both (CO_2) treatments (**Supplementary Figure S6**), indicating that the higher *A* observed in both ILs is mostly driven by specific changes at the photobiochemistry level (**Figure 5**).

In silico Expression Analysis of Genes From BIN 2K

Based on leaf expression data from a recent study (Ranjan et al., 2016), we examined the BIN 2K differentially expressed genes in

leaves from IL 2–5 and IL 2–6 plants (**Supplementary Table S2**). We observed that a subset of 30 genes were differentialy expressed in the ILs in comparison with M82. Out of 30 genes, nine were upregulated while 19 genes were downregulated only in IL 2–5. Regarding the IL 2–6, three genes were upregulated and 11 negatively regulated. We also verified that three genes were upregulated in plants from both ILs namely an AMP-activated protein kinase (Solyc02g091530.2.1), a polypeptide inferred from GFF3 feature (Solyc02g091770.1.1), and an adiponectin receptor 2 (Solyc02g092230.2.1). Noteworthy, four genes were strongly downregulated in plants from both IL 2–5 and 2–6 including a transcription factor described as CBF_NF-Y_archaeal histone (Solyc02g090930.2.1), a multidrug resistance protein mdtK from MATE family transporter related proteins (Solyc02g091070.2.1), an epidermal patterning factor-like protein 2 (Solyc02g091910.1.1), and a formamidase-like protein (Solyc02g092530.2.1). It is important to mention, however, that caution should be taken as not to over−interpret this comparison given that the RNAseq information was obtained from an entirely independent experiment and solely for leaves.

DISCUSSION

Given our previous demonstration that CO_2 assimilation rates of both ILs 2–5 and 2–6 plants were on average 20% higher compared to M82 (de Oliveira Silva et al., 2018), we decided to deeper investigate the physiological mechanisms responsible for their enhanced CO_2 assimilation. After evaluating photosynthetic parameters, we observed that both ILs exhibited substantially higher A (∼22%), and ETR under high (CO_2; **Table 2**), whereas no alterations were observed under ambient (CO_2) in the lines compared to their respective M82. Regarding photosynthetic results under ambient (CO_2), it is well established that modulations of photosynthesis mainly occur in response to environmental factors including light and temperature. In fact, the conditions of the current experiment were characterized by higher temperatures and light intensities in comparison with those previously described (de Oliveira Silva et al., 2018). Possibly, such conditions led to higher P_r (∼12 μmol CO_2 m^{-2} s^{-1}; **Table 1**) than those previously observed for ILs (∼8 μmol CO_2 m^{-2} s^{-1}; de Oliveira Silva et al., 2018). As a result, even with an increased V_{cmax} and J_{max} (and, consequently, A_{gross}), increases in A could not be observed in the ILs at ambient (CO_2), as the lower C_c led to higher P_r under these conditions (**Table 1**). Nevertheless, the two ILs exhibited increased levels of RuBisCO, while only IL 2–5 displayed significantly higher protein content under ambient (CO_2; **Figure 3**). Increased protein levels can be overall associated with higher V_{cmax} values providing an important source of variation in carbon uptake capacity (Hikosaka, 2004) and it is in agreement with the elevated biomass production and total leaf area of the ILs (**Figures 1A,H**).

The increased photosynthesis in the ILs under high (CO_2) could be explained, at least partially, by higher ETR values (**Table 2**). Considering that the regeneration of RuBP is determinant of the limitation of A under high (CO_2; Mitchell et al., 2000), even small increments in photochemical components (e.g., ETR) may have resulted in higher photosynthetic activity in the ILs (**Figure 5**). The manipulation of the photosynthetic electron transport chain has been proposed as a valuable tool to enhance the carbon assimilation in plants (Simkin et al., 2017b, 2019). In agreement, transgenic Arabidopsis and tobacco plants expressing algal Cytochrome c_6 gene exhibited increase in ETR, A as well as chlorophyll and starch contents, and further increment in biomass production (Chida et al., 2007; Yadav et al., 2018).

Close association between carbon and nitrogen metabolisms has been demonstrated in plants (Foyer et al., 1998; Araújo et al., 2008; Gauthier et al., 2010). Thus, any alteration in carbon abundance is expected to reflect in nitrogen levels (Gutschick, 1999; Nunes-Nesi et al., 2010). Among the metabolites measured in plants under elevated (CO_2), chlorophyll and protein accumulated in the IL 2–5 as well as starch in leaves from both ILs (**Figures 6A–C**), which must be interpreted in light of photosynthetic data. Chlorophyll is an important part of the light-dependent reactions, and it is responsible for light harvesting during photosynthesis, therefore it has been considered an important predictor of photosynthetic potential (Croft et al., 2017; Liu et al., 2019). In its turn, the higher A was determining for the increased starch content, without, however, leading to the retroinhibition of the photosynthetic process (**Figure 6C**). In good agreement, the high protein levels of ILs could mean a higher demand for proteins involved in the metabolism and export of carbohydrates resulting from the higher photosynthetic rate.

Based both on the available leaf expression data (Chitwood et al., 2013; Ranjan et al., 2016) and in our previously published work (de Oliveira Silva et al., 2018), we verified that several genes are differentially expressed in the IL 2–5 and IL 2–6. In addition to genes mentioned here (**Supplementary Table S2**), three other genes appears as potential candidates involved in the responses that lead to higher photosynthetic performance observed in the ILs 2–5 and 2–6, namely the ATP−dependent Clp protease (Solyc02g091280), NADH dehydrogenase iron–sulfur protein 4 (Solyc02g092270), and beta subunit of an ATP synthase (Solyc02g091130; de Oliveira Silva et al., 2018). The proteins encoded by these genes are largely involved in energy metabolism and therefore might be involved with photosynthetic capacity. Moreover, genes enconding proteins related with photosynthesis, chlorophyll biosynthesis, and response to light stimulus were also upregulated mainly in the IL 2–5 (Ranjan et al., 2016). Noteworthy, the candidate genes for the higher photosynthetic capacity observed in plants from ILs 2–5 and 2–6 (**Supplementary Table S2**; and de Oliveira Silva et al., 2018) should be further investigated in more details. In this regard, introgression sublines with introgressed fragments smaller than the original set of ILs (Alseekh et al., 2013) are an alternative to reduce genetic variance and the amount of genes to be further analyzed; consequently, shortening the detection of the genes influencing photosynthetic capacity in tomato plants.

By analyzing the effects of the genetic variation on chromosome 2 of ILs 2–5 and 2–6 that modulates the upregulation of photosynthetic capacity, we have here provided

novel insights into the mechanisms that govern photosynthetic capacity in tomato. Considering the higher values of J_{max} in ILs under ambient (CO_2), followed by the enhanced *A* and ETR values in ILs exposed to elevated (CO_2), it seems reasonable to assume that both ILs optimize their investment in the components involved in RuBP regeneration. Thus, genetic manipulation in these components may be an opportunity to increase photosynthesis reflecting positively on growth in a future environment with high (CO_2; Ding et al., 2016; Driever et al., 2017; Simkin et al., 2017b), or currently in greenhouses that employ CO_2 fertilization to improve productivity (Mortensen, 1987). Noteworthy, considering that the control of the CO_2 assimilation in the Calvin–Benson cycle is shared among several enzymes, an increase in photosynthetic potential could be achieved combining multigene manipulation (Raines, 2003; Simkin et al., 2019). Recent studies demonstrated that increasing simultaneously the activity of different enzymes of the C3 cycle in the same plant resulted in an increased CO_2 fixation and biomass yield dramatically (Simkin et al., 2015, 2017a). Recent challenges associated with an engineering improved photosynthesis leading to the optimized utilization of CO_2 to maximize crop production have been discussed elsewhere (Batista-Silva et al., 2020). In this regard, the *S. pennellii* ILs population represents an opportunity to explore the large quantity of traits that affect plant survival as well as yield potential once ILs facilitate the identification of large number of genes affecting single or several plant phenotypes. Perhaps more importantly, our findings not only open up a novel fundamental research avenue, given that they identify a genomic region that lead to significant enhanced photosynthetic capacity, but also have important biotechnological implications, specifically with regard to the potential for increased yield, without increasing the need for arable land.

DATA AVAILABILITY STATEMENT

All datasets generated for this study are included in the article/**Supplementary Material**.

AUTHOR CONTRIBUTIONS

AN-N designed the research. JL-C, FO, and DC characterized the introgression lines under supervision of AN-N and WA. JL-C, WB-S, and RS performed the Western blot analyses. AN-N, FO, and JG analyzed the data. JL-C and AN-N wrote the manuscript with input from all the other authors. JG, DM, SM, and WA complemented the writing.

FUNDING

Financial support was provided by Conselho Nacional de Desenvolvimento Científico e Tecnológico (CNPq; grant numbers 306818/2016-7, 402511/2016-6, and 424024/2018-7), Fundação de Amparo à Pesquisa do Estado de Minas Gerais (FAPEMIG; grant numbers BPD-00019-16 to FO, and RED-00053-16), and Max Planck Society to AN-N and WA.

ACKNOWLEDGMENTS

Research fellowships granted by CNPq to AN-N and WA as well as the scholarship granted by the Brazilian Federal Agency for Support and Evaluation of Graduate Education (CAPES-Brazil) to WB-S are also gratefully acknowledged.

SUPPLEMENTARY MATERIAL

The Supplementary Material for this article can be found online at: https://www.frontiersin.org/articles/10.3389/fpls.2020.00794/full#supplementary-material

REFERENCES

Ainsworth, E. A., and Rogers, A. (2007). The response of photosynthesis and stomatal conductance to rising [CO2]: mechanisms and environmental interactions. *Plant. Cell Environ.* 30, 258–270. doi: 10.1111/j.1365-3040.2007.01641.x

Alseekh, S., Ofner, I., Pleban, T., Tripodi, P., Di Dato, F., Cammareri, M., et al. (2013). Resolution by recombination: breaking up *Solanum pennellii* introgressions. *Trends Plant Sci.* 18, 536–538. doi: 10.1016/j.tplants.2013.08.003

Araújo, W. L., Nunes-Nesi, A., Trenkamp, S., Bunik, V. I., and Fernie, A. R. (2008). Inhibition of 2-oxoglutarate dehydrogenase in potato tuber suggests the enzyme is limiting for respiration and confirms its importance in nitrogen assimilation. *Plant Physiol.* 148, 1782–1796. doi: 10.1104/pp.108.126219

Asín, M. J. (2002). Present and future of quantitative trait locus analysis in plant breeding. *Plant Breed.* 121, 281–291. doi: 10.1046/j.1439-0523.2002.730285.x

Batista-Silva, W., da Fonseca-Pereira, P., Oliveira Martins, A., Zsögön, A., Nunes-Nesi, A., and Araújo, W. L. (2020). Engineering improved photosynthesis in the era of synthetic biology. *Plant Commun.* 1, 1–17. doi: 10.1016/j.xplc.2020.100032

Bradford, M. M. (1976). A rapid and sensitive method for the quantitation of microgram quantities of protein utilizing the principle of protein-dye binding. *Anal. Biochem.* 72, 248–254. doi: 10.1016/0003-2697(76)90527-90523

Brandt, S., Fachinger, S., Tohge, T., Fernie, A. R., Braun, H. P., and Hildebrandt, T. M. (2018). Extended darkness induces internal turnover of glucosinolates in *Arabidopsis thaliana* leaves. *PLoS One* 13:e0202153. doi: 10.1371/journal.pone.0202153

Causse, M., Duffe, P., Gomez, M. C., Buret, M., Damidaux, R., Zamir, D., et al. (2004). A genetic map of candidate genes and QTLs involved in tomato fruit size and composition. *J. Exp. Bot.* 55, 1671–1685. doi: 10.1093/jxb/erh207

Chida, H., Nakazawa, A., Akazaki, H., Hirano, T., Suruga, K., Ogawa, M., et al. (2007). Expression of the algal cytochrome c6 gene in *Arabidopsis* enhances photosynthesis and growth. *Plant Cell Physiol.* 48, 948–957. doi: 10.1093/pcp/pcm064

Chitwood, D. H., Kumar, R., Headland, L. R., Ranjan, A., Covington, M. F., Ichihashi, Y., et al. (2013). A quantitative genetic basis for leaf morphology in a set of precisely defined tomato introgression lines. *Plant Cell* 25, 2465–2481. doi: 10.1105/tpc.113.112391

Croft, H., Chen, J. M., Luo, X., Bartlett, P., Chen, B., and Staebler, R. M. (2017). Leaf chlorophyll content as a proxy for leaf photosynthetic capacity. *Glob. Chang. Biol.* 23, 3513–3524. doi: 10.1111/gcb.13599

Cross, J. M., von Korff, M., Altmann, T., Bartzetko, L., Sulpice, R., Gibon, Y., et al. (2006). Variation of enzyme activities and metabolite levels in 24 Arabidopsis accessions growing in carbon-limited conditions. *Plant Physiol.* 142, 1574–1588. doi: 10.1104/pp.106.086629

Cruz, C. D. (2013). GENES - a software package for analysis in experimental statistics and quantitative genetics. *Acta Sci.* 35, 271–276. doi: 10.4025/actasciagron.v35i3.21251

De Kauwe, M. G., Lin, Y.-S., Wright, I. J., Medlyn, B. E., Crous, K. Y., Ellsworth, D. S., et al. (2016). A test of the "one-point method" for estimating maximum carboxylation capacity from field-measured, light-saturated photosynthesis. *New Phytol.* 210, 1130–1144. doi: 10.1111/nph.13815

de Oliveira Silva, F. M., Lichtenstein, G., Alseekh, S., Rosado-Souza, L., Conte, M., Suguiyama, V. F., et al. (2018). The genetic architecture of photosynthesis and plant growth-related traits in tomato. *Plant Cell Environ.* 41, 327–341. doi: 10.1111/pce.13084

Ding, F., Wang, M., Zhang, S., and Ai, X. (2016). Changes in SBPase activity influence photosynthetic capacity, growth, and tolerance to chilling stress in transgenic tomato plants. *Sci. Rep.* 6:32741. doi: 10.1038/srep32741

Dreyer, E., Roux, X. L., Montpied, P., Dauded, F., and Masson, F. (2001). Temperature response of leaf photosynthetic capacity in seedlings from seven temperate tree species. *Tree Physiol.* 21, 223–232. doi: 10.1093/treephys/21.4.223

Driever, S. M., Lawson, T., Andralojc, P. J., Raines, C. A., and Parry, M. A. J. (2014). Natural variation in photosynthetic capacity, growth, and yield in 64 field-grown wheat genotypes. *J. Exp. Bot.* 65, 4959–4973. doi: 10.1093/jxb/eru253

Driever, S. M., Simkin, A. J., Alotaibi, S., Fisk, S. J., Madgwick, P. J., Sparks, C. A., et al. (2017). Increased sbpase activity improves photosynthesis and grain yield in wheat grown in greenhouse conditions. *Philos. Trans. R. Soc. B Biol. Sci.* 372:384. doi: 10.1098/rstb.2016.0384

Eshed, Y., and Zamir, D. (1995). An introgression line population of Lycopersicon pennellii in the cultivated tomato enables the identification and fine mapping of yield-associated QTL. *Genetics* 141, 1147–1162.

Ethier, G. J., and Livingston, N. J. (2004). On the need to incorporate sensitivity to CO2 transfer conductance into the farquhar-von caemmerer-berry leaf photosynthesis model. *Plant Cell Environ.* 27, 137–153. doi: 10.1111/j.1365-3040.2004.01140.x

Evans, J. R. (2013). Improving photosynthesis. *Plant Physiol.* 162, 1780–1793. doi: 10.1104/pp.113.219006

Evans, J. R., and Poorter, H. (2001). Photosynthetic acclimation of plants to growth irradiance: the relative importance of specific leaf area and nitrogen partitioning in maximizing carbon gain. *Plant, Cell Environ.* 24, 755–767. doi: 10.1046/j.1365-3040.2001.00724.x

Fanourakis, D., Giday, H., Milla, R., Pieruschka, R., Kjaer, K. H., Bolger, M., et al. (2015). Pore size regulates operating stomatal conductance, while stomatal densities drive the partitioning of conductance between leaf sides. *Ann. Bot.* 115, 555–565. doi: 10.1093/aob/mcu247

Farquhar, G. D., and Sharkey, T. D. (1982). Stomatal conductance and photosynthesis. *Annu. Rev. Plant Physiol.* 33, 317–345. doi: 10.1146/annurev.pp.33.060182.001533

Farquhar, G. D., von Caemmerer, S., and Berry, J. A. (1980). A biochemical model of photosynthetic CO2 assimilation in leaves of C3 species. *Planta* 149, 78–90. doi: 10.1007/BF00386231

Fernie, A. R., Roscher, A., Ratcliffe, R. G., and Kruger, N. J. (2001). Fructose 2,6-bisphosphate activates pyrophosphate: fructose-6-phosphate 1-phosphotransferase and increases triose phosphate to hexose phosphate cycling in heterotrophic cells. *Planta* 212, 250–263. doi: 10.1007/s004250000386

Flexas, J., Barbour, M. M., Brendel, O., Cabrera, H. M., Carriquí, M., Díaz-Espejo, A., et al. (2012). Mesophyll diffusion conductance to CO2: an unappreciated central player in photosynthesis. *Plant Sci.* 193-194, 70–84. doi: 10.1016/J.PLANTSCI.2012.05.009

Flexas, J., and Carriquí, M. (2020). Photosynthesis and photosynthetic efficiencies along the terrestrial plant's phylogeny: lessons for improving crop photosynthesis. *Plant J.* 101, 964–978. doi: 10.1111/tpj.14651

Flexas, J., Diaz-Espejo, A., Galmés, J., Kaldenhoff, R., Medrano, H., and Ribas-Carbo, M. (2007). Rapid variations of mesophyll conductance in response to changes in CO 2 concentration around leaves. *Plant Cell Environ.* 30, 1284–1298. doi: 10.1111/j.1365-3040.2007.01700.x

Flood, P. J., Harbinson, J., and Aarts, M. G. M. (2011). Natural genetic variation in plant photosynthesis. *Trends Plant Sci.* 16, 327–335. doi: 10.1016/j.tplants.2011.02.005

Foyer, C. H., Valadier, M.-H., Migge, A., and Becker, T. W. (1998). Drought-induced effects on nitrate reductase activity and mRNA and on the coordination of nitrogen and carbon metabolism in maize leaves. *Plant Physiol.* 117, 283–292. doi: 10.1104/PP.117.1.283

Galle, A., Florez-sarasa, I., Tomas, M., Pou, A., Medrano, H., and Ribas-carbo, M. (2009). The role of mesophyll conductance during water stress and recovery in tobacco (*Nicotiana sylvestris*): acclimation or limitation? *Cell* 60, 2379–2390. doi: 10.1093/jxb/erp071

Galmés, J., Conesa, M. A., Ochogavía, J. M., Perdomo, J. A., Francis, D. M., Ribas-Carbó, M., et al. (2011). Physiological and morphological adaptations in relation to water use efficiency in mediterranean accessions of *Solanum lycopersicum*. *Plant Cell Environ.* 34, 245–260. doi: 10.1111/j.1365-3040.2010.02239.x

Galmés, J., Kapralov, M. V., Andralojc, P. J., Conesa, M. À, Keys, A. J., Parry, M. A. J., et al. (2014). Expanding knowledge of the *Rubisco kinetics* variability in plant species: environmental and evolutionary trends. *Plant Cell Environ.* 37, 1989–2001. doi: 10.1111/pce.12335

Gauthier, P. P. G., Bligny, R., Gout, E., Mahé, A., Nogués, S., Hodges, M., et al. (2010). In folio isotopic tracing demonstrates that nitrogen assimilation into glutamate is mostly independent from current CO2 assimilation in illuminated leaves of *Brassica napus*. *New Phytol.* 185, 988–999. doi: 10.1111/j.1469-8137.2009.03130.x

Geber, M. A., and Dawson, T. E. (1997). Genetic variation in stomatal and biochemical limitations to photosynthesis in the annual plant, *Polygonum arenastrum*. *Oecologia* 109, 535–546. doi: 10.1007/s004420050114

Genty, B., Briantais, J.-M., and Baker, N. R. (1989). The relationship between the quantum yield of photosynthetic electron transport and quenching of chlorophyll fluorescence. *Biochim. Biophys. Acta Gen. Subj.* 990, 87–92. doi: 10.1016/S0304-4165(89)80016-80019

Gong, P., Zhang, J., Li, H., Yang, C., Zhang, C., Zhang, X., et al. (2010). Transcriptional profiles of drought-responsive genes in modulating transcription signal transduction, and biochemical pathways in tomato. *J. Exp. Bot.* 61, 3563–3575. doi: 10.1093/jxb/erq167

Gonzalez-Martinez, S. C., Krutovsky, K. V., and Neale, D. B. (2006). Forest-tree population genomics and adaptive evolution. *New Phytol.* 170, 227–238. doi: 10.1111/j.1469-8137.2006.01686.x

Grassi, G., and Magnani, F. (2005). Stomatal, mesophyll conductance and biochemical limitations to photosynthesis as affected by drought and leaf ontogeny in ash and oak trees. *Plant Cell Environ.* 28, 834–849. doi: 10.1111/j.1365-3040.2005.01333.x

Gu, J., Yin, X., Struik, P. C., Stomph, T. J., and Wang, H. (2012). Using chromosome introgression lines to map quantitative trait loci for photosynthesis parameters in rice (*Oryza sativa* L.) leaves under drought and well-watered field conditions. *J. Exp. Bot.* 63, 455–469. doi: 10.1093/jxb/err292

Gutschick, V. P. (1999). Research reviews biotic and abiotic consequences of differences in leaf structure. *New Phytol.* 143, 3–18. doi: 10.1046/j.1469-8137.1999.00423.x

Harley, P. C., Loreto, F., Marco, G., and Sharkey, T. D. (1992). Theoretical considerations when estimating the mesophyll conductance to CO2 flux by analysis of the response of photosynthesis to CO2. *Plant Physiol.* 98:1429. doi: 10.1104/pp.98.4.1429

Hermida-Carrera, C., Kapralov, M. V., and Galmés, J. (2016). Rubisco catalytic properties and temperature response in crops 1. *Plant Physiol.* 171, 2549–2561. doi: 10.1104/pp.16.01846

Hikosaka, K. (2004). Interspecific difference in the photosynthesis - nitrogen relationship: patterns, physiological causes, and ecological importance. *J. Plant Res.* 117, 481–494. doi: 10.1007/s10265-004-0174-172

Hunt, R., Causton, D. R., Shipley, B., and Askew, A. P. (2002). A modern tool for classical plant growth analysis. *Ann. Bot.* 90, 485–488. doi: 10.1093/AOB/MCF214

Jamil, M., Ali, A., Akbar, K. F., Napar, A. A., and Gul, A. (2016). *QTL Analysis in Plants: Ancient and Modern Perspectives*. Berlin: Springer International Publishing.

Lefebvre, S., Lawson, T., Fryer, M., Zakhleniuk, O. V., Lloyd, J. C., and Raines, C. A. (2005). Increased sedoheptulose-1,7-bisphosphatase activity in transgenic tobacco plants stimulates photosynthesis and growth from an early stage in development 1. *Plant Physiol.* 138, 451–460. doi: 10.1104/pp.104.055046

Liu, C., Liu, Y., Lu, Y., Liao, Y., Nie, J., Yuan, X., et al. (2019). Use of a leaf chlorophyll content index to improve the prediction of above-ground biomass and productivity. *PeerJ* 6:e6240. doi: 10.7717/peerj.6240

Logan, B. A., Adams, W. W., and Demmig-Adams, B. (2007). Avoiding common pitfalls of chlorophyll fluorescence analysis under field conditions. *Funct. Plant Biol.* 34, 853–859. doi: 10.1071/FP07113

Long, S. P., Ainsworth, E. A., Rogers, A., and Ort, D. R. (2004). Rising atmospheric carbon dioxide: plants FACE the future. *Annu. Rev. Plant Biol.* 55, 591–628. doi: 10.1146/annurev.arplant.55.031903.141610

Mitchell, R. A. C., Theobald, J. C., and Lawlor, D. W. (2000). Is there scope for improving balance between RuBP-regeneration and carboxylation capacities in wheat at elevated CO2? *J. Exp. Bot.* 51, 391–397. doi: 10.1093/jexbot/51.suppl_1.391

Miyagawa, Y., Tamoi, M., and Shigeoka, S. (2001). Overexpression of a cyanobacterial fructose-1,6-/sedoheptulose-1,7-bisphosphatase in tobacco enhances photosynthesis and growth. *Nat. Biotechnol.* 19, 965–969. doi: 10.1038/nbt1001-965

Mortensen, L. (1987). Review: CO2 enrichment in greenhouses. *Crop Responses. Sci. Hortic.* 33, 1–25. doi: 10.1016/0304-4238(87)90028-8

Mott, K. A. (1988). Do stomata respond to CO2 concentrations other than intercellular? *Plant Physiol.* 86, 200–203. doi: 10.1104/pp.86.1.200

Muir, C. D., Pease, J. B., and Moyle, L. C. (2014). Quantitative genetic analysis indicates natural selection on leaf phenotypes across wild tomato species (*Solanum sect. lycopersicon; solanaceae*). *Genetics* 198, 1629–1643. doi: 10.1534/genetics.114.169276

Nuccio, M. L., Potter, L., Stiegelmeyer, S. M., Curley, J., Cohn, J., Wittich, P. E., et al. (2017). Strategies and tools to improve crop productivity by targeting photosynthesis. *Philso. Trans. R. Soc. B* 372:20160377. doi: 10.1098/rstb.2016.0377

Nunes-Nesi, A., Carrari, F., Gibon, Y., Sulpice, R., Lytovchenko, A., Fisahn, J., et al. (2007). Deficiency of mitochondrial fumarase activity in tomato plants impairs photosynthesis via an effect on stomatal function. *Plant J.* 50, 1093–1106. doi: 10.1111/j.1365-313X.2007.03115.x

Nunes-Nesi, A., Fernie, A. R., and Stitt, M. (2010). Metabolic and signaling aspects underpinning the regulation of plant carbon nitrogen interactions. *Mol. Plant* 3, 973–996. doi: 10.1093/mp/ssq049

Nunes-Nesi, A., Nascimento, V. D. L., De Oliveira Silva, F. M., Zsögön, A., Araújo, W. L., and Sulpice, R. (2016). Natural genetic variation for morphological and molecular determinants of plant growth and yield. *J. Exp. Bot.* 67, 2989–3001. doi: 10.1093/jxb/erw124

Ort, D. R., Merchant, S. S., Alric, J., Barkan, A., Blankenship, R. E., Bock, R., et al. (2015). Redesigning photosynthesis to sustainably meet global food and bioenergy demand. *PNAS* 112, 8529–8536. doi: 10.1073/pnas.1424031112

Parry, M. A. J., Andralojc, P. J., Scales, J. C., Salvucci, M. E., Carmo-Silva, A. E., Alonso, H., et al. (2013). Rubisco activity and regulation as targets for crop improvement. *J. Exp. Bot.* 64, 717–730. doi: 10.1093/jxb/ers336

Peterhansel, C., Horst, I., Niessen, M., Blume, C., Kebeish, R., Kürkcüoglu, S., et al. (2010). Photorespiration. *Arab. B* 8:e0130. doi: 10.1199/tab.0130

Pons, T. L., Flexas, J., Caemmerer, S., Von Evans, J. R., Genty, B., Ribas-carbo, M., et al. (2009). Estimating mesophyll conductance to CO2: methodology, potential errors, and recommendations. *J. Exp. Bot.* 60, 2217–2234. doi: 10.1093/jxb/erp081

Porra, R. J., Thompson, W. A., and Kriedemann, P. E. (1989). Determination of accurate extinction coefficients and simultaneous equations for assaying chlorophylls a and b extracted with four different solvents: verification of the concentration of chlorophyll standards by atomic absorption spectroscopy. *Biochim. Biophys. Acta Bioenerg.* 975, 384–394. doi: 10.1016/S0005-2728(89)80347-80340

Raines, C. A. (2003). The calvin cycle revisited. *Photosynth. Res.* 75, 1–10. doi: 10.1023/A:1022421515027

Ranjan, A., Budke, J. M., Rowland, S. D., Chitwood, D. H., Kumar, R., Carriedo, L., et al. (2016). eQTL regulating transcript levels associated with diverse biological processes in tomato. *Plant Physiol.* 172, 328–340. doi: 10.1104/pp.16.00289

Rebetzke, G. J., Rattey, A. R., Farquhar, G. D., Richards, R. A., and Condon, A. G. (2013). Genomic regions for canopy temperature and their genetic association with stomatal conductance and grain yield in wheat. *Funct. Plant Biol.* 40:14. doi: 10.1071/FP12184

Semel, Y., Nissenbaum, J., Menda, N., Zinder, M., Krieger, U., Issman, N., et al. (2006). Overdominant quantitative trait loci for yield and fitness in tomato. *Proc. Natl. Acad. Sci. U.S.A.* 103, 12981–12986. doi: 10.1073/pnas.0604635103

Sharkey, T. D., Bernacchi, C. J., Farquhar, G. D., and Singsaas, E. L. (2007). Fitting photosynthetic carbon dioxide response curves for C 3 leaves. *Plant. Cell Environ.* 30, 1035–1040. doi: 10.1111/j.1365-3040.2007.01710.x

Simkin, A. J., Lopez-Calcagno, P. E., Davey, P. A., Headland, L. R., Lawson, T., Timm, S., et al. (2017a). Simultaneous stimulation of sedoheptulose 1,7-bisphosphatase, fructose 1,6-bisphophate aldolase and the photorespiratory glycine decarboxylase-H protein increases CO2 assimilation, vegetative biomass and seed yield in *Arabidopsis*. *Plant Biotechnol. J.* 15, 805–816. doi: 10.1111/pbi.12676

Simkin, A. J., Mcausland, L., Lawson, T., and Raines, C. A. (2017b). Overexpression of the RieskeFeS protein increases electron transport rates and biomass yield 1 [CC-BY]. *Science* 175, 134–145. doi: 10.1104/pp.17.00622

Simkin, A. J., López-Calcagno, P. E., Raines, C. A., and Lunn, J. E. (2019). Feeding the world: improving photosynthetic efficiency for sustainable crop production. *J. Exp. Bot.* 70, 1119–1140. doi: 10.1093/jxb/ery445

Simkin, A. J., Mcausland, L., Headland, L. R., Lawson, T., and Raines, C. A. (2015). Multigene manipulation of photosynthetic carbon assimilation increases CO2 fixation and biomass yield in tobacco. *J. Exp. Bot.* 66, 4075–4090. doi: 10.1093/jxb/erv204

Singh, J., Pandey, P., James, D., Chandrasekhar, K., Achary, V. M. M., Kaul, T., et al. (2014). Enhancing C3 photosynthesis: an outlook on feasible interventions for crop improvement. *Plant Biotechnol. J.* 12, 1217–1230. doi: 10.1111/pbi.12246

Sulpice, R., Pyl, E.-T., Ishihara, H., Trenkamp, S., Steinfath, M., Witucka-Wall, H., et al. (2009). Starch as a major integrator in the regulation of plant growth. *Proc. Natl. Acad. Sci. U.S.A.* 106, 10348–10353. doi: 10.1073/pnas.0903478106

Tiranti, V., Viscomi, C., Hildebrandt, T., Di Meo, I., Mineri, R., Tiveron, C., et al. (2009). Loss of ETHE1, a mitochondrial dioxygenase, causes fatal sulfide toxicity in ethylmalonic encephalopathy. *Nat. Med.* 15, 200–205. doi: 10.1038/nm.1907

Towbin, H., Staehelin, T., and Gordon, J. (1979). Electrophoretic transfer of proteins from polyacrylamide gels to nitrocellulose sheets: procedure and some applications. *Proc. Natl. Acad. Sci. U.S.A.* 76, 4350–4354. doi: 10.1073/pnas.76.9.4350

Valentini, R., Epron, D., de Angelis, P., Matteucci, G., and Dreyer, E. (1995). In situ estimation of net CO2 assimilation, photosynthetic electron flow and photorespiration in Turkey oak (*Q. cerris* L.) leaves: diurnal cycles under different levels of water supply. *Plant. Cell Environ.* 18, 631–640. doi: 10.1111/j.1365-3040.1995.tb00564.x

Vasconcelos, ÉA. R., Nogueira, F. C. S., Abreu, E. F. M., Gonçalves, E. F., Souza, P. A. S., and Campos, F. A. P. (2005). Protein extraction from cowpea tissues for 2-D Gel electrophoresis and MS analysis. *Chromatographia* 62, 447–450. doi: 10.1365/s10337-005-0637-631

von Caemmerer, S. (2000). *Biochemical Models Of Leaf Photosynthesis*. Clayton: CSIRO Publishing.

von Caemmerer, S., and Farquhar, G. D. (1981). Some relationships between the biochemistry of photosynthesis and the gas exchange of leaves. *Planta* 153, 376–387. doi: 10.1007/BF00384257

Vrabl, D., Vas Kova, M., Hronkova, M., Flexas, J., Antru, C., and Ek, J. S. (2009). Mesophyll conductance to CO2 transport estimated by two independent methods: effect of variable CO2 concentration and abscisic acid. *J. Exp. Bot.* 60, 2315–2323. doi: 10.1093/jxb/erp115

Walker, A. P., Beckerman, A. P., Gu, L., Kattge, J., Cernusak, L. A., Domingues, T. F., et al. (2014). The relationship of leaf photosynthetic traits - *V* cmax and

J max - to leaf nitrogen, leaf phosphorus, and specific leaf area: a meta-analysis and modeling study. *Ecol. Evol.* 4, 3218–3235. doi: 10.1002/ece3.1173

Xu, X., Martin, B., Comstock, J. P., Vision, T. J., Tauer, C. G., Zhao, B., et al. (2008). Fine mapping a QTL for carbon isotope composition in tomato. *Theor. Appl. Genet.* 117, 221–233. doi: 10.1007/s00122-008-0767-766

Yadav, S. K., Khatri, K., Rathore, M. S., and Jha, B. (2018). Introgression of UfCyt c 6, a thylakoid lumen protein from a green seaweed *Ulva fasciata* Delile enhanced photosynthesis and growth in tobacco. *Mol. Biol. Rep.* 45, 1745–1758. doi: 10.1007/s11033-018-4318-4311

Yemm, E. W., Cocking, E. C., and Ricketts, R. E. (1955). The determination of amino-acids with ninhydrin. *Analyst* 80:209. doi: 10.1039/AN9558000209

Conflict of Interest: The authors declare that the research was conducted in the absence of any commercial or financial relationships that could be construed as a potential conflict of interest.